OPEN

# Passive Cycle Training Promotes Bone Recovery after Spinal Cord Injury without Altering Resting-State Bone Perfusion

JOSHUA F. YARROW[1,2,3], RUSSELL D. WNEK[1], CHRISTINE F. CONOVER[1], MICHAEL C. REYNOLDS[1], KINLEY H. BUCKLEY[1], JAYACHANDRA R. KURA[1], TOMMY W. SUTOR[1], DANA M. OTZEL[2], ALEX J. MATTINGLY[4], STEPHEN E. BORST[4], SUMMER M. CROFT[5], J. IGNACIO AGUIRRE[5], DARREN T. BECK[6], and DANIELLE J. MCCULLOUGH[7]

*[1]Research Service, Malcom Randall Department of Veterans Affairs Medical Center, North Florida/South Georgia Veterans Health System, Gainesville, FL; [2]Brain Rehabilitation Research Center, Malcom Randall Department of Veterans Affairs Medical Center, North Florida/South Georgia Veterans Health System, Gainesville, FL; [3]Division of Endocrinology, Diabetes, and Metabolism, University of Florida College of Medicine, Gainesville, FL; [4]Geriatrics Research, Education, and Clinical Center, North Florida/South Georgia Veterans Health System, Gainesville, FL; [5]Department of Physiological Sciences, University of Florida College of Veterinary Medicine, Gainesville, FL; [6]Department of Cell Biology and Physiology, Edward Via College of Osteopathic Medicine – Auburn Campus, Auburn, AL; and [7]Department of Medical Education, Edward Via College of Osteopathic Medicine – Auburn Campus, Auburn, AL*



**ABSTRACT**

YARROW, J. F., R. D. WNEK, C. F. CONOVER, M. C. REYNOLDS, K. H. BUCKLEY, J. R. KURA, T. W. SUTOR, D. M. OTZEL, A. J. MATTINGLY, S. E. BORST, S. M. CROFT, J. I. AGUIRRE, D. T. BECK, and D. J. MCCULLOUGH. Passive Cycle Training Promotes Bone Recovery after Spinal Cord Injury without Altering Resting-State Bone Perfusion. *Med. Sci. Sports Exerc.*, Vol. 55, No. 5, pp. 813–823, 2023. **Introduction:** Spinal cord injury (SCI) produces diminished bone perfusion and bone loss in the paralyzed limbs. Activity-based physical therapy (ABPT) modalities that mobilize and/or reload the paralyzed limbs (e.g., bodyweight-supported treadmill training (BWSTT) and passive-isokinetic bicycle training) transiently promote lower-extremity blood flow (BF). However, it remains unknown whether ABPT alter resting-state bone BF or improve skeletal integrity after SCI. **Methods:** Four-month-old male Sprague-Dawley rats received $T_9$ laminectomy alone (SHAM; $n = 13$) or $T_9$ laminectomy with severe contusion SCI ($n = 48$). On postsurgery day 7, SCI rats were stratified to undergo 3 wk of no ABPT, quadrupedal (q)BWSTT, or passive-isokinetic hindlimb bicycle training. Both ABPT regimens involved two 20-min bouts per day, performed 5 $d \cdot wk^{-1}$. We assessed locomotor recovery, bone turnover with serum assays and histomorphometry, distal femur bone microstructure using *in vivo* microcomputed tomography, and femur and tibia resting-state bone BF after *in vivo* microsphere infusion. **Results:** All SCI animals displayed immediate hindlimb paralysis. SCI without ABPT exhibited uncoupled bone turnover and progressive cancellous and cortical bone loss. qBWSTT did not prevent these deficits. In comparison, hindlimb bicycle training suppressed surface-level bone resorption indices without suppressing bone formation indices and produced robust cancellous and cortical bone recovery at the distal femur. No bone BF deficits existed 4 wk after SCI, and neither qBWSTT nor bicycle altered resting-state bone perfusion or locomotor recovery. However, proximal tibia BF correlated with several histomorphometry-derived bone formation and resorption indices at this skeletal site across SCI groups. **Conclusions:** These data indicate that passive-isokinetic bicycle training reversed cancellous and cortical bone loss after severe SCI through antiresorptive and/or bone anabolic actions, independent of locomotor recovery or changes in resting-state bone perfusion. **Key Words:** UNLOADING, DISUSE, VASCULAR, EXERCISE, MUSCULOSKELETAL

Address for correspondence: Joshua F. Yarrow, M.S., Ph.D., North Florida/South Georgia Veterans Health System, 1601 SW Archer Road, Research 151, Gainesville, FL 32608-1197; E-mail: Joshua.Yarrow@medicine.ufl.edu.

Submitted for publication August 2022.
Accepted for publication November 2022.
Supplemental digital content is available for this article. Direct URL citations appear in the printed text and are provided in the HTML and PDF versions of this article on the journal's Web site (www.acsm-msse.org).

0195-9131/23/5505-0813/0
MEDICINE & SCIENCE IN SPORTS & EXERCISE®


DOI: 10.1249/MSS.0000000000003101

Severe spinal cord injury (SCI) predisposes persons to rapid sublesional bone loss (1) and profound fracture risk that worsens in the paralyzed limbs throughout the duration of musculoskeletal unloading (2). These bone deficits are impacted by the neural insult and the resulting paralysis and may be worsened by other factors (3), including diminished bone blood flow (BF) in the impaired limbs (4). In this regard, reduced femur and tibia BF temporally coincides with bone loss in our SCI model, with the most pronounced bone BF deficits existing at the distal femur where bone loss is most severe (5). Moreover, distal femur BF was positively correlated with distal femur cancellous volumetric bone mineral density (BMD), cortical bone area (Ct.Ar), and cortical bone area fraction (Ct.Ar/T.Ar) acutely after SCI (5), suggesting that bone BF may influence skeletal preservation in the paralyzed limbs in a site-specific manner.

Activity-based physical therapy (ABPT) modalities that mobilize and/or reload the paralyzed limbs (e.g., bodyweight-supported treadmill training (BWSTT) or passive limb movements) increase BF in the impaired extremities (6–8) and may improve muscle recovery (9). Various ABPT regimens have also been promoted as a means to increase BMD after SCI (10), as intermittent loading with high peak strains or high strain rates increases BMD in neurologically intact persons (11). However, well-controlled trials evaluating the influence of ABPT on BMD in persons with SCI have produced inconsistent results, especially when assessing the distal femur and proximal tibia sites that are most prone to fracture in this population (10). Preclinical ABPT modalities (e.g., quadrupedal (q)BWSTT and passive-isokinetic bicycle training) also promote hindlimb locomotor and neuromuscular recovery in rodent mild-to-moderate SCI models (12,13), although their ability to alter bone remodeling, improve skeletal integrity, and influence bone perfusion in the paralyzed limbs remains to be discerned.

The purposes of this study were to 1) determine the effects of qBWSTT and passive-isokinetic bicycle training on bone turnover, cancellous and cortical microstructure, and resting-state bone BF in our rat severe SCI model and 2) evaluate associations between resting-state bone perfusion and surface-level bone turnover indices after SCI. We hypothesized that 1) SCI would produce progressive bone loss due to increased bone resorption and suppressed bone formation, 2) our ABPT regimens would attenuate bone loss and promote resting-state bone perfusion in the paralyzed limbs via antiresorptive and/or bone anabolic actions, and 3) resting-state bone perfusion would be associated with surface-level bone turnover indices.

## METHODS

**Animal care.** Barrier-raised and specific-pathogen-free 4-month-old male Sprague-Dawley rats (Charles River, Wilmington, MA) were individually housed in a temperature–/light-controlled room (12-h light/dark cycles) and fed rodent chow (Teklad Global 18% Protein Rodent Diet; Harlan, Indianapolis, IN) and tap water *ad libitum*. Procedures conformed to the ILAR Guide to the Care and Use of Experimental Animals and were approved by the Institutional Animal Care and Use Committee at North Florida/South Georgia Veterans Health System.

**Experimental design.** Rats were randomized to receive $T_9$ laminectomy alone (SHAM; $n = 13$) or laminectomy with severe SCI ($n = 41$). On postsurgery day 7, SCI rats with qualifying Basso–Beattie–Bresnahan (BBB) scores were stratified based on locomotor recovery (described hereinafter) to undergo 3 wk of no ABPT ($n = 13$), qBWSTT ($n = 12$), or passive-isokinetic bicycle (Cycle) training ($n = 16$). Open-field locomotion was assessed weekly via the BBB scale (14). Blood was sampled weekly from the tail vein to track whole-body bone turnover. *In vivo* microcomputed tomography (microCT) was used to track distal femur cancellous and cortical bone microstructure. Declomycin and calcein (15 $mg \cdot kg^{-1}$ SC) were administered to fluorochrome label bone formation sites 10 and 3 d before sacrifice, respectively. At 4 wk after surgery, femur and tibia BF was determined in conscious (awake) rats using the *in vivo* microsphere infusion method (5). Animals were euthanized by thoracotomy and terminal exsanguination via cardiac puncture under isoflurane, with femurs and tibias excised and analyzed, as described hereinafter.

**Animal model rationale.** We used skeletally mature male rats because most SCI occur in adult men (3). Severe contusion SCI was selected because this model mimics the most common pathologic mechanism of severe traumatic SCI in humans and produces immediate and persistent hindlimb paralysis and extensive bone deficits (15,16). In comparison, mild-to-moderate SCI models recover the ability to support the hindlimbs in stance and to perform stepping and do not typically display bone loss (17).

**Surgery and postoperative care.** Surgery and postoperative care were performed per our methods (5,15,16,18–22). Briefly, anesthetized rats received $T_9$ laminectomy alone (SHAM surgery), which involved surgical isolation and removal of the $T_9$ spinous process to expose the spinal cord, or $T_9$ laminectomy with severe (250 kdyne) contusion SCI using the Infinite Horizons Impactor (PSI, Lexington, KY). All rats received ketoprofen (5.0 $mg \cdot kg^{-1}$ SC) and buprenorphine (0.05 $mg \cdot kg^{-1}$ SC) for 48 h and ampicillin for 5 d. Rats were housed in recovery units that were placed partially on and partially off water-circulating heat pads throughout the study to assist in body temperature maintenance. Postsurgery care included daily examination for signs of pain/distress, weight loss, dehydration, fecal clearance, skin lesions, bladder dysfunction, and joint mobility. Bladders were expressed twice daily until spontaneous voiding returned, which typically occurred within 2 wk after surgery. Lactated Ringer's was provided to promote rehydration. Jell-O with added protein/fat, Froot Loops®, and apple slices were given to assist in body mass recovery.

**Verification of SCI severity.** We used *a priori* criteria to exclude rats that displayed locomotor recovery inconsistent with severe SCI, as previously reported (5,15), because residual hindlimb function impedes bone loss after SCI independent of therapeutic intervention (16). Our approach was developed by assessing BBB scores in several hundred male rats

that received severe SCI (5,16,18–22) and identifying animals that spontaneously regained the ability to support their hindlimbs in stance and/or performed weight-supported hindlimb stepping (BBB >9). Specifically, on day 7 post-SCI, we excluded rats that displayed BBB scores >4, when averaging hindlimbs, or >7 in either hindlimb. All remaining rats were stratified based on BBB score to undergo no ABPT, qBWSTT, or passive-isokinetic Cycle training, ensuring homogenous locomotor function among groups at day 7.

**ABPT protocols.** qBWSTT and Cycle training were initiated on day 7 post-SCI and involved training 40 min·d$^{-1}$, 5 d·wk$^{-1}$ for 3 wk. For qBWSTT, rats were suspended by a harness that provided 40% bodyweight support, with the paralyzed hindlimbs manually positioned into plantar stepping positions on the treadmill (3.5 m·min$^{-1}$, or ~20–25 strides per minute), per our protocol (22). For Cycle, rats were suspended from a harness that provided 100% bodyweight support, with the hindfeet strapped to motor-driven pedals that produced passive-isokinetic cycling motions in the paralyzed hindlimbs (~6 rotations per minute), as previously reported (12,13). On training day 1, rats were given 5 min to explore each device. For acclimation, rats performed four 5-min bouts in the morning, with 5-min rest between bouts, and four 5-min bouts in the afternoon, with 4- to 5-h rest between sessions. On training day 2, rats performed two 10-min bouts in the morning and afternoon. On all remaining days, rats completed one 20-min bout in the morning and afternoon. Stepping/pedaling rates were progressively increased as rats acclimated to training.

**MicroCT assessment of cancellous and cortical bone microstructure.** *In vivo* microCT was performed 1–3 d before surgery and at 2 and 4 wk after surgery, using a Bruker Skyscan 1176 (Kontich, Belgium), per our methods (5). Briefly, rats were anesthetized via isoflurane and secured on the scanning bed with the left leg extended to optimize image acquisition at the distal femur. Images were acquired at 80 kVP/311 μA, with both 0.45-mm-thick Cu and a 0.5-mm Al filter, 2000 × 1336-pixel resolution, 18.0-μm voxel, 0.5° rotation step, and 180° tomographic rotation (scan time ~10 min, anesthesia duration ~16 min). Images were reconstructed in NRecon (v1.7.4.6, all software Bruker Skyscan) and rotated/aligned in DataViewer (v1.6.0.0). Volumes of interest (VOI) were developed and analyzed in CTAn (v1.17.7.2). The cancellous VOI began 1.5 mm proximal to the growth plate at the distal femoral metaphysis and extended 4.0 mm in the proximal direction. The cortical VOI encompassed the most proximal one-third (1.333 mm) of the cancellous VOI, which completely avoided the residual growth plate that interferes with the assessment of cortical bone. All microCT outcomes are reported as percentage change from baseline. Cancellous outcomes included the following: trabecular bone volume (BV/TV; in percent), trabecular number (Tb.N; numbers per millimeter), trabecular thickness (Tb.Th; in millimeters), trabecular separation (Tb.Sp; in millimeters), and connectivity density (Conn.D; in numbers per cubic millimeter). Cortical outcomes included the following: total bone and medullary area (T.Ar; in squared millimeters), Ct.Ar (in squared millimeters), and Ct.Ar/T.Ar (in percent).

**Histomorphometry assessment of bone microstructure and surface-level bone turnover indices.** Cancellous microstructure and bone turnover indices were evaluated at the left proximal tibial metaphysis, as previously reported (15). In brief, tibiae were fixed in 10% phosphate-buffered formalin, dehydrated in ethanol, and embedded undecalcified in methyl methacrylate. To assess cancellous structure, 4-μm-thick sections were stained with von Kossa and counterstained with tetrachrome (Polysciences, Warrington, PA). To measure fluorochrome-based bone formation indices, 8-μm-thick sections remained unstained. The region of interest began 0.5 mm distal to the growth plate and excluded the primary spongiosa and cancellous bone within 0.25 mm of the endocortical border. Outcomes measured by the OsteoMeasure System (Osteometrics, Decatur, GA) included the following: cancellous BV/TV (in percent), Tb.N (in numbers per millimeter), Tb.Th (in micrometers), Tb.Sp (in micrometers), number of osteoblasts and osteoclasts per cancellous perimeter (in numbers per millimeter), eroded bone surface (ES/BS; in percent), single-labeled surface (sLS/BS; in percent), double-labeled surfaces (dLS/BS; in percent %), mineralizing surface (MS/BS, %), mineral apposition rate (MAR; in micrometers per day), and bone formation rate (BFR/BS; in cubic micrometers per squared micrometer per day). MS/BS, an index of active bone formation, was calculated as dLS/BS plus one-half of the sLS/BS divided by total bone surface [((dLS/BS + 0.5(sLs/BS))/BS]. MAR, an index of osteoblastic activity, was calculated by dividing the interlabel distance by the time between fluorochrome labels. BFR/BS was calculated by multiplying dLS/BS and MAR. These outcomes conform to recommendations of the ASBMR Histomorphometry Nomenclature Committee (23).

**Circulating bone turnover markers.** Enzyme immunoassays were used to determine circulating tartrate-resistant acid phosphatase 5b (TRAPC5b) and procollagen type 1 N-terminal propeptide (P1NP) as whole-body bone resorption and formation markers, respectively (IDS, Scottsdale, AZ). Bone turnover markers are reported as percentage change from baseline.

**Bone BF assessments.** *In vivo* resting-state bone BF was determined in conscious (awake) rats via the microsphere infusion technique, which requires surgical implantation of fluid filled (sterile, heparinized saline) catheters into the left ventricle of the heart (via the carotid artery) and the tail (via the caudal artery) for microsphere infusion and reference blood sampling, respectively (5). Briefly, 3 d after concluding ABPT, catheters were surgically implanted into the carotid and caudal arteries of anesthetized rats. Placement in the left ventricle was confirmed by retrograde BF into the catheter. The catheters were externalized and secured to the skin, and surgical incisions were closed. After 4-h recovery, awake rats were secured, and 1-mL heparinized saline was administered into each catheter. Next, 15-μm colored (UV; yellow) polystyrene microspheres (~$10^6$ spheres, DyeTrak VII+; Triton Technology) were infused via the carotid catheter, with the line flushed to ensure clearance of sphere. A reference blood sample was acquired via the caudal catheter via a withdrawal-infusion pump (GenieTouch, Kent Scientific) at 0.35 mL·min$^{-1}$ for 1 min after microsphere

infusion. Rats were then euthanized, and bones dissected, weighed, and cut cross-sectionally into proximal, midshaft (diaphysis), and distal segments. Tissue digestion and microsphere recovery were performed on the reference blood sample, bilateral femur segments, and right tibia segments, per the sedimentation method (5). After microsphere extraction and reconstitution, supernatant was assessed with UV spectrophotometry (440 and 670 nm). BF was calculated with the DyeTrak VII+ matrix inversion program. After verification of equal distribution to left and right hindlimbs, BF was averaged across contralateral bones, when available, and reported as milliliters per minute per gram for whole bones and for each bone segment.

**Statistical analysis.** One-way ANOVA and repeated-measures ANOVA were used to evaluate outcomes assessed at single or multiple time points, respectively, with Tukey's *post hoc* tests performed when appropriate (SPSS v26.0.0; IBM). Data distribution was assessed with the Kolmogorov–Smirnov test. Consistency in bilateral BF was verified with paired-samples *t*-tests and Pearson correlation coefficients. Associations between proximal tibial BF and proximal tibial bone turnover indices were assessed with Pearson correlation coefficients across all SCI groups, with the Holm–Bonferonni correction used to control type 1 error. Results are reported as means ± SEM (for actual values) or estimated marginal means ± SEM (for percent change from baseline), with $P < 0.05$ as the threshold of significance.

## RESULTS

No baseline differences were observed among groups, and no differences in impact force or velocity used to produce the contusion SCI, via the IH impactor, were present among the SCI cohorts (Supplemental Table 1, Supplemental Digital Content, Presurgical body mass and injury characteristics, bone microstructural parameters, and serum bone turnover markers, http://links.lww.com/MSS/C771).

**Animal recovery.** All SCI rats displayed immediate postsurgical hindlimb paralysis. On day 7 post-SCI, $n = 8$ SCI rats were removed for exceeding *a priori* criteria (1-wk BBB score = 6.2 ± 0.6). Another rat was excluded after experiencing a distal femur fracture of unknown origin with radiographically visible callous formation impairing joint mobility. These animals were replaced to ensure similar group allocations. All SHAM rats maintained BBB scores of 21 throughout, and no signs of pain, distress, or abnormal behavior were observed. Group and time main effects for BBB and body mass are presented in Supplemental Table 2 (Supplemental Digital Content, Statistical outcomes and treatment effects for variables assessed at multiple time points, http://links.lww.com/MSS/C771), with interactions revealing that all SCI groups had lower BBB scores and greater body mass loss versus SHAM and compared with baseline at all postsurgical time points ($P < 0.01$; Figs. 1A, B). Neither ABPT regimen improved BBB score.

**MicroCT assessment of cancellous and cortical bone microstructure.** Representative images of cancellous and cortical bone within the VOI are presented in Figures 2 and 3, respectively. Group and/or time main effects existed for all cancellous and cortical outcomes (Supplemental Table 2, Supplemental Digital Content, Statistical outcomes and treatment effects for variables assessed at multiple time points, http://links.lww.com/MSS/C771). For cancellous bone (Figs. 2A–E), interactions revealed that the SCI no-ABPT group exhibited robust BV/TV and Tb.N deficits and lower Conn.D at 2 wk (all $P < 0.01$ vs SHAM) and continual bone loss thereafter. This was evidenced by lower BV/TV, Tb.N, and Tb.Th, and higher Tb.Sp at 4 wk (all $P < 0.01$ vs SCI 2 wk and for SCI vs SHAM at 4 wk). qBWSTT did not prevent these deficits or alter the trajectory of bone loss over either period. In comparison, Cycle attenuated the reduction in Conn.D during the initial 2 wk ($P < 0.05$ vs SCI and SCI + qBWSTT), without preventing other SCI-induced cancellous bone deficits. From 2 to 4 wk, Cycle increased BV/TV by completely preserving Tb.N and by concomitantly increasing Tb.Th ~20% over this period, resulting in increased Conn.D (all $P < 0.01$, 4 vs 2 wk). Ultimately, SCI + Cycle displayed percentage change values for BV/TV, Tb.N, and Conn.D that were not different from SHAM ($P < 0.01$ vs SCI and SCI + qBWSTT), along with a 15%–25% greater Tb.Th increase versus all other groups ($P < 0.01$).

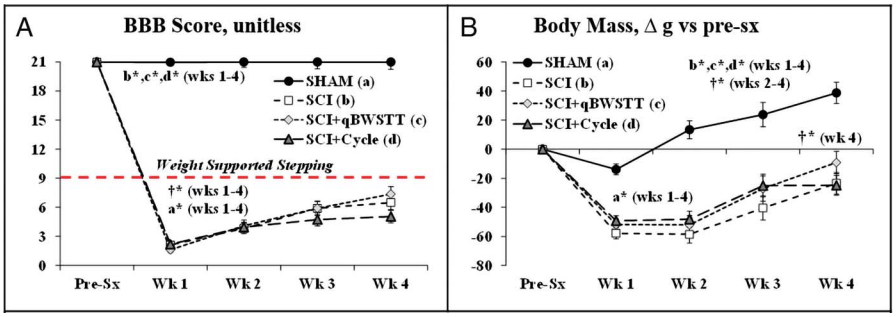


**FIGURE 1—A and B, BBB locomotor rating scores and body mass change from before surgery (pre-sx) in rats that received $T_9$ laminectomy alone (SHAM), $T_9$ laminectomy plus SCI, SCI with qBWSTT (SCI + qBWSTT), or SCI with passive-isokinetic bicycle training (SCI + Cycle). Values are estimated marginal means ± SEM, $n = 12$–16/group. Some error bars are within the size of the symbol. † indicates difference vs pre-sx, and letters indicate difference vs respectively labeled groups (a = vs SHAM, b = vs SCI, c = vs SCI + qBWSTT, and d = vs SCI + Cycle) at $P < 0.05$ or $*P < 0.01$. Note: *Horizontal dashed line* (A) indicates the threshold for voluntary overground weight-supported plantar stepping (i.e., BBB ≥ 9). SCI animals that exceeded *a priori* criteria were excluded before analysis. Complete statistical findings are in Supplemental Table 2 (Supplemental Digital Content, Statistical outcomes and treatment effects for variables assessed at multiple time points, http://links.lww.com/MSS/C771).**

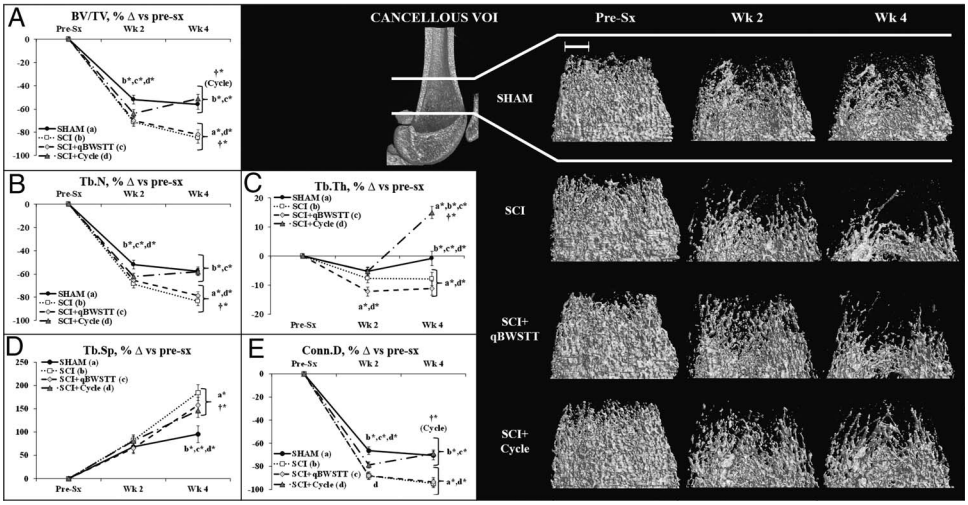


**FIGURE 2—A–E, Cancellous bone microstructural data (A–E) and representative cancellous bone images (*right panel*) at the distal femoral metaphysis cancellous VOI acquired via *in vivo* microCT before surgery (pre-sx) and 2 and 4 wk after rats received $T_9$ laminectomy (SHAM), $T_9$ laminectomy plus SCI, SCI plus qBWSTT (SCI + qBWSTT), or SCI plus passive-isokinetic bicycle training (SCI + Cycle). Values are estimated marginal means ± SEM of the percent change from pre-sx, *n* = 11–15/group. Some error bars are within the size of the symbol. † indicates within-group difference for 2 vs 4 wk. Letters indicate difference vs respectively labeled groups (a = vs SHAM, b = vs SCI, c = vs SCI + qBWSTT, and d = vs SCI + Cycle) at $P < 0.05$ or $*P < 0.01$. Scale bar, 1 mm. Complete statistical findings in Supplemental Table 2 (Supplemental Digital Content, Statistical outcomes and treatment effects for variables assessed at multiple time points, http://links.lww.com/MSS/C771).**

For cortical bone (Figs. 3A–C), interactions revealed that all SCI groups displayed lower Ct.Ar and Ct.Ar/T.Ar versus SHAM at 2 wk (both $P < 0.01$), regardless of the intervention. Thereafter, the SCI no-ABPT group displayed ongoing cortical loss, evidenced by reduced T.Ar ($P < 0.01$, 4 vs 2 wk) and relatively stable Ct.Ar over this period, producing an apparent Ct.Ar/T.Ar increase ($P < 0.01$). From 2 to 4 wk, qBWSTT attenuated the SCI-induced T.Ar loss but did not alter Ct.Ar, resulting in lower Ct.Ar/T.Ar versus SCI at 4 wk ($P < 0.01$). Cycle also attenuated the T.Ar reduction from 2 to 4 wk and concomitantly increased Ct.Ar, producing 15% higher Ct.Ar/T.Ar (both $P < 0.01$, 4 vs 2 wk). Ultimately, SCI + Cycle exhibited more cortical bone recovery than other SCI groups, evidenced by higher percentage increases in T.Ar ($P < 0.01$, vs SCI only), Ct.Ar ($P < 0.01$, vs both), and Ct.Ar/T.Ar ($P < 0.01$, vs both), and a similar Ct.Ar/T.Ar increase to SHAM. However, T.Ar and Ct.Ar both remained lower in SCI + Cycle versus SHAM (both $P < 0.01$).

**Histomorphometry assessment of bone microstructure and surface-level bone turnover indices.** Cancellous bone structural outcomes and cell surface/dynamic histomorphometry findings are presented in Figures 4A–L. SCI displayed

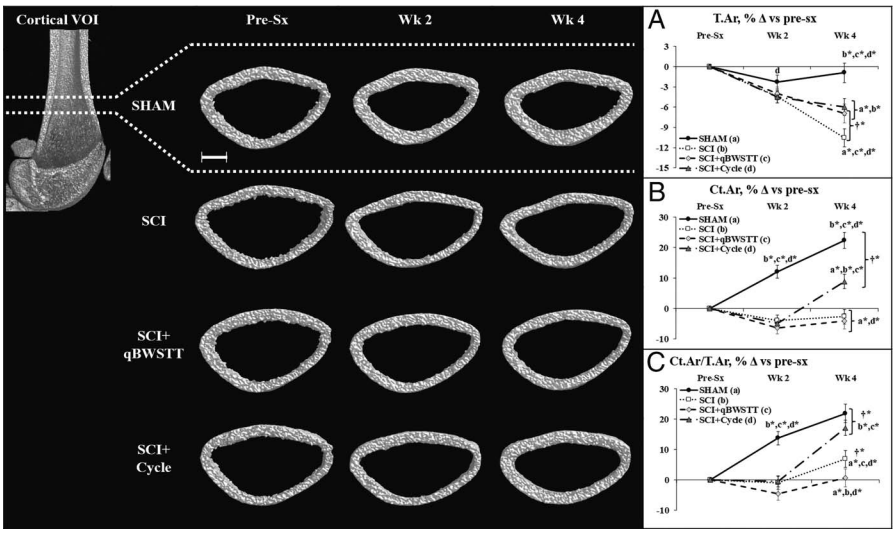


**FIGURE 3—A–C, Representative cortical bone microstructural images (*left panel*) and cortical microstructural data (A–C) at the distal femur cortical VOI acquired via *in vivo* microCT before surgery (pre-sx) and 2 and 4 wk after rats received $T_9$ laminectomy (SHAM), $T_9$ laminectomy plus SCI, SCI plus qBWSTT (SCI + qBWSTT), or SCI plus passive-isokinetic bicycle training (SCI + Cycle). Values are estimated marginal means ± SEM of the percent change from pre-sx, *n* = 11–15/group. Some error bars are within the size of the symbol. † indicates within-group difference for 2 vs 4 wk. Letters indicate difference vs respectively labeled groups (a = vs SHAM, b = vs SCI, c = vs SCI + qBWSTT, and d = vs SCI + Cycle) at $P < 0.05$ or $*P < 0.01$. Scale bar, 1 mm. Complete statistical findings are in Supplemental Table 2 (Supplemental Digital Content, Statistical outcomes and treatment effects for variables assessed at multiple time points, http://links.lww.com/MSS/C771).**

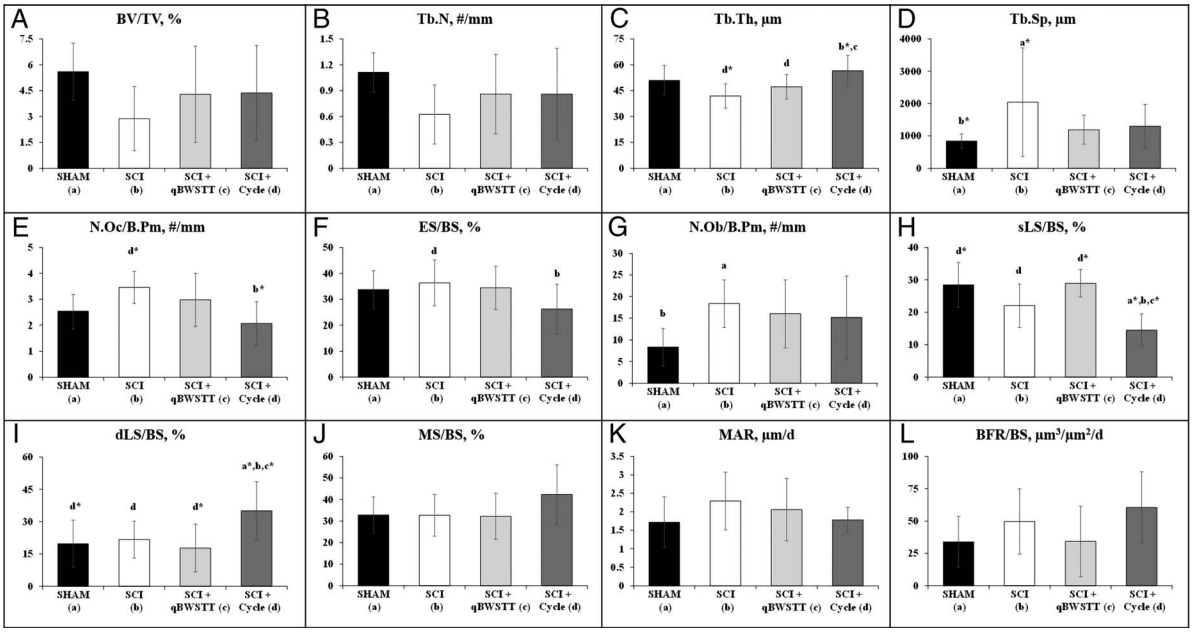


**FIGURE 4—A–L, Cancellous bone microstructural and cell surface data and dynamic bone turnover indices assessed via histomorphometry at the proximal tibial metaphysis 4 wk after surgery in rats that received $T_9$ laminectomy (SHAM), $T_9$ laminectomy plus SCI, SCI plus qBWSTT (SCI + qBWSTT), or SCI plus motorized passive-isokinetic bicycle training (SCI + Cycle). Values are Means ± SD, $n$ = 9–15/group. Letters indicate differences vs respectively labeled groups (a = vs SHAM, b = vs SCI, c = vs SCI + qBWSTT, and d = vs SCI + Cycle) at $P < 0.05$ or $*P < 0.01$.**

45%–50% lower proximal tibia BV/TV and Tb.N and ~20% lower Tb.Th versus SHAM (all nonsignificant), along with higher Tb.Sp ($P < 0.01$) and number of osteoblasts per cancellous bone perimeter (N.Ob/B.Pm; $P < 0.05$) versus SHAM. SCI + qBWSTT exhibited no histomorphometric differences when compared with SCI or SHAM. In comparison, SCI + Cycle exhibited 10%–35% higher Tb.Th versus SCI ($P < 0.01$) and SCI + qBWSTT ($P < 0.05$), lower number of osteoclasts per cancellous bone perimeter (N.Oc/B.Pm; $P < 0.01$) and ES/BS ($P < 0.05$) versus SCI, and lower sLS/BS and 60%–100% higher dLS/BS versus all other groups (both $P < 0.05$–$<0.01$). N.Ob/B.Pm and BFR/BS were also ~80% higher (directionally) in SCI + Cycle versus SHAM, although these and other surface-based bone formation indices did not achieve statistical significance.

**Circulating bone turnover markers.** Group and time main effects existed for circulating TRAPC5b and P1NP (Supplemental Table 2, Supplemental Digital Content, Statistical outcomes and treatment effects for variables assessed at multiple time points, http://links.lww.com/MSS/C771). Group effects indicated that all SCI groups displayed higher TRAPC5b versus SHAM ($P < 0.001$), with interactions revealing that larger TRAPC5b percentage increases for all SCI groups versus SHAM at both 1 and 2 wk and for SCI + qBWSTT versus SHAM at 3 wk (Fig. 5A, $P < 0.05$–$0.01$). In addition, group effects indicated that the P1NP decrease from baseline was greater for SCI and SCI + Cycle versus SHAM and SCI + qBWSTT (Fig. 5B).

**Bone BF assessments.** *In vivo* resting-state bone perfusion was highly correlated between contralateral femurs ($r = 0.905$,

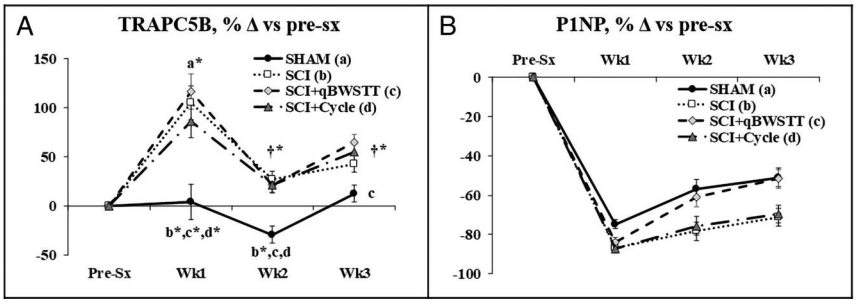


**FIGURE 5—A and B, TRAPC5B (whole-body bone resorption marker) and P1NP (whole-body bone formation marker) assessed before surgery (pre-sx) and 1, 2, and 3 wk after rats received $T_9$ laminectomy (SHAM), $T_9$ laminectomy plus SCI, SCI plus qBWSTT (SCI + qBWSTT), or SCI plus passive-isokinetic bicycle training (SCI + Cycle). Values are estimated marginal means ± SEM of the percent change from baseline, $n$ = 11–12/group. Some error bars are within the size of the symbol. † indicates within-group difference vs 1 wk. Letters indicate difference vs respectively labeled groups (a = vs SHAM, b = vs SCI, c = vs SCI + qBWSTT, and d = vs SCI + Cycle) at $P < 0.05$ or $*P < 0.01$. Note: Values are not available at 4 wk because the colored microspheres present within the circulation (necessary to assess bone BF) interfered with colorimetric assays. Complete statistical findings are in Supplemental Table 2 (Supplemental Digital Content, Statistical outcomes and treatment effects for variables assessed at multiple time points, http://links.lww.com/MSS/C771).**

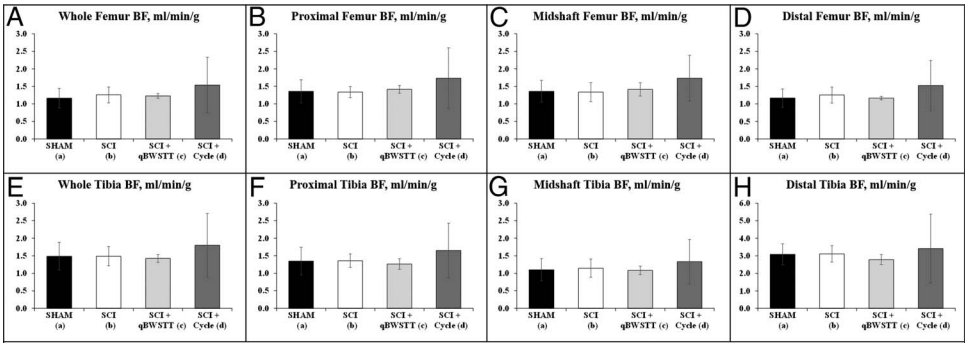


**FIGURE 6—A–H, Resting-state bone BF determined in the whole bones and the proximal, midshaft, and distal regions of the femurs (A–D) and tibia (E–H) in unanesthetized (awake) rats via the microsphere infusion technique. BF was assessed 4 wk after surgery in rats that received $T_9$ laminectomy (SHAM), $T_9$ laminectomy plus SCI, SCI plus qBWSTT (SCI + qBWSTT), or SCI plus motorized passive-isokinetic bicycle training (SCI + Cycle). Note: Resting-state BF was assessed 3 to 4 d after cessation of qBWSTT or Cycle. Values are means ± SD, $n$ = 9–11/group. No differences were present among groups, although SCI + Cycle displayed the highest resting-state bone BF at all sites evaluated.**

$P < 0.001$) with no differences in right versus left femur perfusion within any group (data not shown), indicating bilateral symmetry in bone BF distribution. However, resting-state femur and tibia BF was not different across groups when assessed 3 d after the conclusion of training. Regardless, whole bone and region-specific femur and tibia perfusion were 10%–30% higher (directionally) in SCI + Cycle versus all other groups (Figs. 6A–H).

Across all SCI groups, associations existed between proximal tibia BF and the following histomorphometry-derived proximal tibia bone formation and resorption indices: dLS/BS ($r$ = 0.560, $P$ = 0.003), MS/BS ($r$ = 0.505, $P$ = 0.009), BFR/BS ($r$ = 0.464, $P$ = 0.022), and ES/BS ($r$ = −0.479, $P$ = 0.013; Figs. 7A–F). Proximal tibia BF was also associated with proximal tibia Tb.Th across all SCI cohorts ($r$ = 0.480,

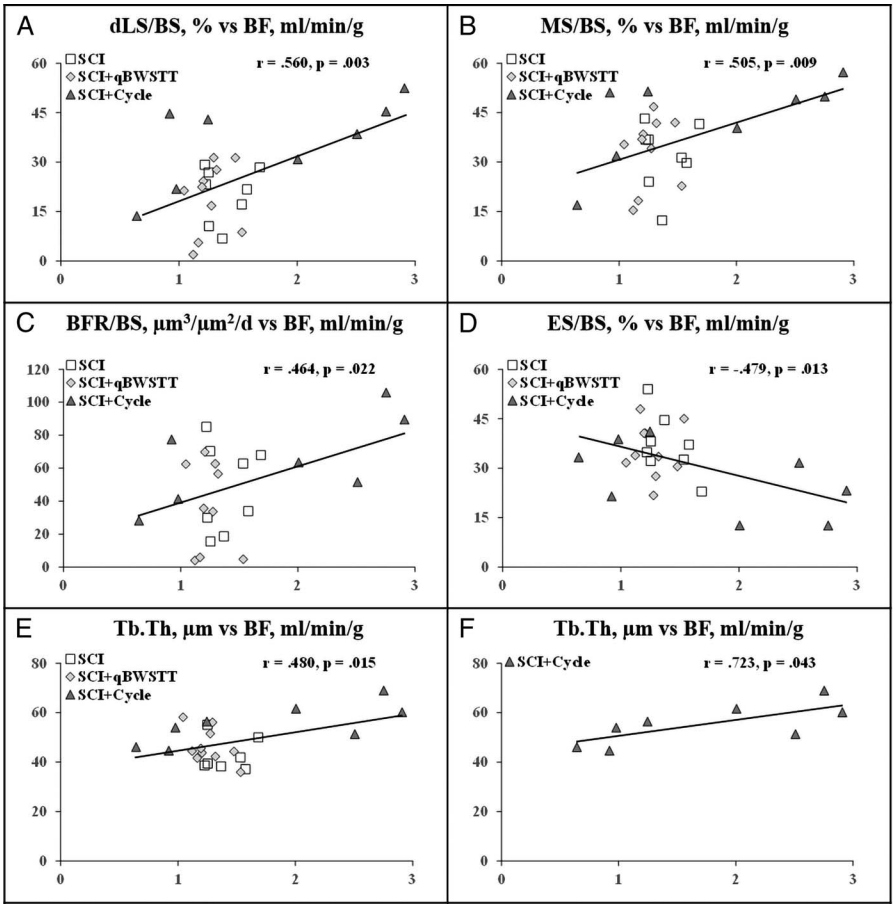


**FIGURE 7—A–F, Comparison of proximal tibia BF and histomorphometry-derived bone turnover and bone structural indices at the proximal tibia in rats that received $T_9$ laminectomy plus SCI, SCI plus qBWSTT (SCI + qBWSTT), or SCI plus passive-isokinetic bicycle training (SCI + Cycle). Values reported for individual animals, $n$ = 8–9/group. Note: BF is on the horizontal $x$ axis, and histomorphometry-derived bone outcomes are on the vertical $y$ axis.**

$P = 0.015$) and within the SCI + Cycle group ($r = 0.723$, $P = 0.043$; Figs. 7A–F).

## DISCUSSION

SCI produces extensive cancellous and cortical bone loss at the distal femur and proximal tibia (24,25), which worsens fracture risk at these sites (2). This bone loss is influenced by disuse resulting from the neurologic insult and perhaps by other factors (3), such as reduced bone BF in the paralyzed limbs acutely after SCI (5). ABPT modalities that mobilize and/or reload the paralyzed limbs transiently increase lower-extremity BF (6–8) and improve muscular recovery (9). As a result, it has been proposed that certain ABPT may alter bone perfusion (26,27) and promote bone recovery (10), although this remains to be elucidated. Herein, we assessed the effects of qBWSTT and passive-isokinetic Cycle training on bone turnover, bone microstructure, and resting-state bone BF in the paralyzed limbs of our rat severe SCI model. In doing so, we observed increased circulating TRAPC5b (bone resorption marker) and concomitantly reduced P1NP (bone formation marker) throughout the acute (baseline to 2 wk) to subacute (2 to 4 wk) post-SCI phase in the SCI no-ABPT group, concurrent with ongoing cancellous bone loss and persistent cortical bone deficits at the distal femur. qBWSTT did not prevent any SCI-induced bone microstructural deficit at the distal femur, nor did it alter circulating TRAPC5b. In contrast, passive-isokinetic Cycle training 1) completely preserved distal femur Tb.N over the subacute phase and robustly increased Tb.Th from 2 to 4 wk, which restored BV/TV to SHAM levels; 2) improved distal femur cortical bone recovery; and 3) suppressed surface-level bone resorption indices and concomitantly increased dLS/BS, a surface-level bone formation measure. At 4 wk after surgery, no differences in resting-state femur or tibia perfusion were present among groups, although bone BF was directionally highest in the SCI + Cycle group throughout all femur and tibia subregions. Moreover, across SCI groups, proximal tibia BF was positively associated with proximal tibia Tb.Th and with several bone formation indices, and was negatively associated with ES/BS, a bone resorption index. These results indicate that passive-isokinetic Cycle training produced robust antiresorptive actions, without suppressing bone formation, resulting in improved cancellous and cortical bone recovery after severe SCI and suggest that subtle alterations in bone BF may influence bone turnover in the paralyzed limbs.

In several past studies, our laboratory (15,16,19,21,22) and others (28,29) utilized static/dynamic histomorphometry and *ex vivo* microCT to compare bones excised from rodent SCI models and controls. These techniques are common within cross-sectional study designs, although they do not control for heterogeneity in bone turnover or microstructure present in Sprague-Dawley rats (30), nor do they allow determination of the rates of bone loss or bone recovery or account for the possibility that sham surgical interventions impact bone loss, as previously reported (5). To overcome these limitations, we tracked circulating bone turnover markers and cancellous and cortical bone loss throughout the acute to subacute phases using serum assays and *in vivo* microCT, respectively. In doing so, we observed that $T_9$ laminectomy (SHAM surgery) reduced P1NP and produced distal femur cancellous bone loss over the acute phase without altering TRAPC5b, congruent with our previous work (5,15). Regardless, over the acute phase, all SCI groups displayed considerably more cancellous bone loss than SHAM, accompanied by impaired cortical bone gain. These skeletal deficits were driven by a bone remodeling imbalance that favored bone loss, as evidenced by a near doubling of TRACP5b and a concomitant >80% reduction in P1NP in the initial post-SCI week. Similarly, in past studies, our laboratory (5,15) and others (29) used time-course histomorphometry to demonstrate that ongoing bone resorption and a near absence of bone formation coexist in the paralyzed limbs during the acute post-SCI phase, confirming uncoupled bone resorption. The SCI no-ABPT group also exhibited ongoing cancellous bone loss throughout the subacute phase, resulting in fewer and thinner trabeculae (lower Tb.N and Tb.Th), along with a persistently smaller distal femur cross-sectional area that comprised less compact bone. These microstructural changes suggest that profound whole-bone mechanical deficits existed at the distal femur, aligning with previous reports (15,16). Nevertheless, at 4 wk after surgery, we observed similar histomorphometry-derived bone turnover indices in SCI versus SHAM, supporting the observation that uncoupled bone resorption is transient and exists predominantly during the acute post-SCI phase (15).

Comprehensive physical rehabilitation regimens focused on improving recovery after SCI use ABPT modalities to mobilize and/or reload the impaired limbs. Such modalities improve central (31) and peripheral (32) cardiovascular health markers in persons with SCI, produce transient hyperemic responses in the paralyzed limbs (6–8), and improve muscular recovery in both humans (9) and animals (12,13) subsequent to mild/moderate SCI. Moreover, treadmill exercise transiently increases muscle (33) and bone BF (34) in nonneurologically impaired models. However, it is unknown whether ABPT alters bone perfusion after SCI (26,27) or improves bone recovery in paralyzed limbs (10). For example, two studies that used near-infrared spectroscopy to evaluate bone BF in persons with SCI reported no change in proximal tibia perfusion immediately after exercise in response to facilitated plantar flexor exercise (26) or functional electrical stimulation rowing (27), whereas increased bone BF was present in nonneurologically impaired controls. Moreover, meta-analyses and systematic reviews report only sparse evidence to support claims that ABPT improves bone in persons with SCI (35,36), with >50% of studies reporting no BMD improvements (10). The reasons underlying the inconsistent bone adaptations to ABPT are unknown, although many studies used training parameters that were not optimal to increase BMD and assessed heterogeneous populations that included persons of varying ages, SCI severities, and SCI durations (10). To address this, we used *in vivo* microCT to track bone changes at the distal femur in age-/sex-/littermate-matched rats that received severe SCI and that displayed near-identical locomotor deficits before ABPT. We also

ensured that the training frequency, duration, and rest intervals (two 20-min bouts per day, separated by 4- to 5-h rest, performed 5 $d \cdot wk^{-1}$ for 3 wk) were consistent with regimens that improve bone in other models (37). In doing so, we noted that all SCI groups exhibited strikingly similar percentage changes in bone turnover and in the magnitude of cancellous and cortical bone loss over the acute phase, which encompassed the week before ABPT initiation and the ABPT acclimation week. In this regard, it is notable that qBWSTT did not lessen distal femur cancellous or cortical bone loss in the acute or subacute phases, nor did it alter surface-level bone turnover indices or suppress circulating TRAPC5b when compared with SCI. However, circulating P1NP was higher in SCI + qBWSTT versus SCI, primarily because of changes occurring after initiation of qBWSTT, suggesting that other skeletal sites may have responded more favorably to this ABPT. In this regard, several case studies/series and controlled clinical trials reported that partial BWSTT and/or overground walking increased hip and/or spine BMD in persons with SCI (38–40), whereas others suggest no change or worsening BMD at the distal femur or proximal tibia (41,42).

Passive bicycle training has been investigated as a modality to improve BMD in persons with SCI, with mixed results (10), perhaps because of the issues detailed previously. Regardless, passive limb movements transiently increase BF in the paralyzed limbs (6–8) and produce neuromuscular benefits in rodent mild-to-moderate SCI models, including improved locomotor recovery (12,13). We extend these findings by reporting that passive-isokinetic Cycle training prevented the SCI-induced reduction in distal femur Tb.N and robustly increase Tb.Th over the subacute phase, which combined to increase distal femur BV/TV. In addition, Cycle training improved distal femur cortical bone gain in the subacute phase, evidenced by increased Ct.Ar and Ct.Ar/Tt.Ar. Moreover, SCI + Cycle exhibited higher proximal tibia Tb.Th versus SCI and SCI + qBWSTT, indicating that bone improvements were not limited to the distal femur. This bone gain was accompanied by fewer osteoclasts (N.Oc/B.Pm) and less eroded bone surface (lower ES/BS) along the cancellous perimeter versus SCI, providing bone surface–level evidence that Cycle stimulated antiresorptive actions, and by higher dLS/BS and concomitantly lower sLS/BS versus all other groups with all other surface-level bone formation indices residing at SHAM levels, indicating that bone formation was maintained. Notably, these Cycle-induced skeletal adaptations occurred independent of locomotor recovery, given that BBB scores were near-identical across SCI groups and remained below the thresholds to support the hindlimbs in stance and/or perform weight-supported stepping (i.e., BBB ≥9). As such, it is not clear how Cycle training and qBWSTT produced divergent skeletal responses, especially given that training frequency, duration, and rest intervals were matched and that the loading magnitudes (qBWSTT, <40% bodyweight-support vs Cycle, 100% bodyweight-support) were below that needed to prevent bone loss in non-SCI disuse models (43). Given this, it is possible that Cycle training stimulated bone strains at the knee independent of weight bearing, although this remains to be determined. Regardless, our results provide the first direct evidence indicating that passive-isokinetic Cycle training produces robust cancellous and cortical bone recovery after severe SCI by suppressing osteoclast-mediated bone resorption and by concomitantly maintaining osteoblast-mediated bone formation, via yet-to-be-identified mechanisms.

Vascular impairments (44,45) and diminished bone BF (46) have been proposed as factors that might influence disuse-induced bone loss (47). In this regard, persons with severe SCI exhibit reduced femoral artery absolute diameter and reduced maximal perfusion in the femoral artery (4), suggesting that impaired bone perfusion exists in the paralyzed limbs. We previously reported that femur and tibia perfusion was 30%–40% lower in conscious (awake) rats subjected to severe SCI during the acute phase, temporally coinciding with uncoupled bone resorption and the most rapid bone loss in our model and that distal femur perfusion was positively associated with several distal femur bone structural parameters in the acute phase (5). These results suggest that altered bone perfusion may influence bone integrity in the paralyzed limbs. As such, we were surprised that the current study indicated no differences in femur or tibia BF in SHAM versus SCI at 4 wk after surgery, especially considering that Ding et al. (48) reported that mice subjected to spinal cord transection exhibited lower intraosseous vascular volume and vessel diameter at 4 wk after surgery, along with lower vascular endothelial growth factor and CD31 within the circulation. Collectively, these findings suggest that 1) the bone BF and bone turnover deficits in the acute phase are likely transient and that both renormalize relative to SHAM during the subacute phase, and 2) the bone BF reductions that exist in the paralyzed limbs during the acute post-SCI phase may be one factor influencing impaired bone turnover and bone loss or *vice versa*. In support of this, our current results indicate that proximal tibia BF was positively associated with several surface-level dynamic bone formation indices at the same skeletal site and negatively associated with ES/BS, a marker of bone resorption. Similarly, others have reported positive associations between bone formation rate and bone blood vessel area, in nonneurologically impaired rodents (49). Regardless, one area that remains unknown is whether Cycle transiently altered bone BF during training or in the immediate postexercise period, which might underlie the improved bone recovery in response to this ABPT.

Although our results are robust, several limitations merit mention. First, our design did not permit comparison of circulating and surface-level bone turnover indices at 4 wk after surgery because the technique we used to determine BF required infusion of colored microspheres into the circulation, which interfered with spectrophotometric analyses (5). Second, we could not determine bone mechanical characteristics or assess molecular signaling pathways underlying our findings because histomorphometry and microsphere-based BF assessments require embedding/sectioning or destruction of tissue samples. Lastly, we used a SHAM control group to account for the surgical stress required to produce the contusion SCI, and it is unclear how bone loss occurring in response to $T_9$ laminectomy may have influenced resting-state bone BF.

Future studies controlling for these factors are warranted based on our current and past results (5).

## CONCLUSIONS

In summary, we observed rapid cancellous and cortical bone loss in the acute post-SCI phase in our rat severe contusion SCI model and relatively slower bone deficits developing thereafter. The acute phase bone loss was accompanied by unbalanced bone remodeling that favored bone resorption, with no discernable surface-level bone turnover deficits or bone perfusion impairments in the subacute phase. qBWSTT did not attenuate distal femur bone loss after severe SCI, nor did it alter surface-level bone turnover or resting-state bone perfusion in the paralyzed limbs. In comparison, passive-isokinetic Cycle training improved distal femur cancellous and cortical bone parameters by suppressing bone resorption and by concomitantly maintaining bone formation. These Cycle-induced bone improvements occurred in the absence of locomotor recovery and without detectable changes in resting-state bone perfusion in the paralyzed limbs during the subacute phase. Regardless, proximal tibia BF was positively associated with Tb.Th and several proximal tibia dynamic bone formation indices and was negatively associated with ES/BS, an index of surface-level bone resorption. Collectively, our findings provide rationale to identify the physiologic changes and the molecular pathways that regulate bone recovery in response to passive-isokinetic Cycle training and to further explore the relationship(s) between bone BF and bone turnover in the paralyzed limbs after severe SCI.

We thank Prodip K. Bose for allowing the use of the passive-isokinetic bicycle system. This work was supported by the Department of Veterans Affairs Office of Research and Development, Rehabilitation Research and Development Service Merit 1I01RX002447, SPiRE 1I21RX002185, and PECASE No. B9280-O to J. F. Y. and by resources provided by the North Florida/South Georgia Veterans Health System. The work reported herein does not represent the views of the US Department of Veterans Affairs or the US Government.

The authors declare that they have no conflicts of interest. The results of this study are presented clearly, honestly, and without fabrication, falsification, or inappropriate data manipulation, and do not constitute endorsement by the American College of Sports Medicine.

## REFERENCES

1. Dauty M, Perrouin Verbe B, Maugars Y, Dubois C, Mathe JF. Supralesional and sublesional bone mineral density in spinal cord–injured patients. *Bone*. 2000;27(2):305–9.
2. Grassner L, Klein B, Maier D, Buhren V, Vogel M. Lower extremity fractures in patients with spinal cord injury characteristics, outcome and risk factors for non-unions. *J Spinal Cord Med*. 2018;41(6):676–83.
3. Yarrow JF, Cardozo CP. Effects of spinal cord injury and related conditions. In: Zaidi M, editor. *Encyclopedia of Bone Biology*. Oxford: Academic Press; 2021. pp. 429–48.
4. Olive JL, McCully KK, Dudley GA. Blood flow response in individuals with incomplete spinal cord injuries. *Spinal Cord*. 2002;40(12):639–45.
5. Yarrow JF, Wnek RD, Conover CF, et al. Bone loss after severe spinal cord injury coincides with reduced bone formation and precedes bone blood flow deficits. *J Appl Physiol (1985)*. 2021;131(4):1288–99.
6. Phadke CP, Vierira L, Mathur S, Cipriano G Jr, Ismail F, Boulias C. Impact of passive leg cycling in persons with spinal cord injury: a systematic review. *Top Spinal Cord Inj Rehabil*. 2019;25(1):83–96.
7. Ballaz L, Fusco N, Cretual A, Langella B, Brissot R. Acute peripheral blood flow response induced by passive leg cycle exercise in people with spinal cord injury. *Arch Phys Med Rehabil*. 2007;88(4):471–6.
8. Burns KJ, Pollock BS, Stavres J, Kilbane M, Brochetti A, McDaniel J. Passive limb movement intervals results in repeated hyperemic responses in those with paraplegia. *Spinal Cord*. 2018;56(10):940–8.
9. Otzel DM, Lee J, Ye F, Borst SE, Yarrow JF. Activity-based physical rehabilitation with adjuvant testosterone to promote neuromuscular recovery after spinal cord injury. *Int J Mol Sci*. 2018;19(6):1701.
10. Sutor TW, Kura J, Mattingly AJ, Otzel DM, Yarrow JF. The effects of exercise and activity-based physical therapy on bone after spinal cord injury. *Int J Mol Sci*. 2022;23(2):608.
11. Kohrt WM, Bloomfield SA, Little KD, Nelson ME, Yingling VR, American College of Sports Medicine. American College of Sports Medicine Position Stand: physical activity and bone health. *Med Sci Sports Exerc*. 2004;36(11):1985–96.
12. Liu M, Bose P, Walter GA, Thompson FJ, Vandenborne K. A longitudinal study of skeletal muscle following spinal cord injury and locomotor training. *Spinal Cord*. 2008;46(7):488–93.
13. Bose PK, Hou J, Parmer R, Reier PJ, Thompson FJ. Altered patterns of reflex excitability, balance, and locomotion following spinal cord injury and locomotor training. *Front Physiol*. 2012;3:258.
14. Basso DM, Beattie MS, Bresnahan JC. A sensitive and reliable locomotor rating scale for open field testing in rats. *J Neurotrauma*. 1995;12(1):1–21.
15. Otzel DM, Conover CF, Ye F, et al. Longitudinal examination of bone loss in male rats after moderate-severe contusion spinal cord injury. *Calcif Tissue Int*. 2019;104(1):79–91.
16. Yarrow JF, Ye F, Balaez A, et al. Bone loss in a new rodent model combining spinal cord injury and cast immobilization. *J Musculoskelet Neuronal Interact*. 2014;14(3):255–66.
17. Voor MJ, Brown EH, Xu Q, et al. Bone loss following spinal cord injury in a rat model. *J Neurotrauma*. 2012;29(8):1676–82.
18. Phillips EG, Beggs LA, Ye F, et al. Effects of pharmacologic sclerostin inhibition or testosterone administration on soleus muscle atrophy in rodents after spinal cord injury. *PLoS One*. 2018;13(3):e0194440.
19. Yarrow JF, Phillips EG, Conover CF, et al. Testosterone plus finasteride prevents bone loss without prostate growth in a rodent spinal cord injury model. *J Neurotrauma*. 2017;34(21):2972–81.
20. Beggs LA, Ye F, Ghosh P, et al. Sclerostin inhibition prevents spinal cord injury-induced cancellous bone loss. *J Bone Miner Res*. 2015;30(4):681–9.
21. Yarrow JF, Conover CF, Beggs LA, et al. Testosterone dose dependently prevents bone and muscle loss in rodents after spinal cord injury. *J Neurotrauma*. 2014;31(9):834–45.
22. Yarrow JF, Kok HJ, Phillips EG, et al. Locomotor training with adjuvant testosterone preserves cancellous bone and promotes muscle plasticity in male rats after severe spinal cord injury. *J Neurosci Res*. 2020;98(5):843–68.
23. Dempster DW, Compston JE, Drezner MK, et al. Standardized nomenclature, symbols, and units for bone histomorphometry: a 2012 update of the report of the ASBMR Histomorphometry Nomenclature Committee. *J Bone Miner Res*. 2013;28(1):2–17.
24. Edwards WB, Simonian N, Troy KL, Schnitzer TJ. Reduction in torsional stiffness and strength at the proximal tibia as a function of time since spinal cord injury. *J Bone Miner Res*. 2015;30(8):1422–30.
25. Edwards WB, Schnitzer TJ, Troy KL. Bone mineral and stiffness loss at the distal femur and proximal tibia in acute spinal cord injury. *Osteoporos Int*. 2014;25(3):1005–15.
26. Zhang C, Modlesky CM, McCully KK. Measuring tibial hemodynamics and metabolism at rest and after exercise using near-infrared spectroscopy. *Appl Physiol Nutr Metab*. 2021;46(11):1354–62.
27. Draghici AE, Potart D, Hollmann JL, et al. Near infrared spectroscopy for measuring changes in bone hemoglobin content after exercise in individuals with spinal cord injury. *J Orthop Res*. 2018;36(1):183–91.

28. Williams JA, Huesa C, Windmill JFC, et al. Spatiotemporal responses of trabecular and cortical bone to complete spinal cord injury in skeletally mature rats. *Bone Rep*. 2022;16:101592.
29. Morse L, Teng YD, Pham L, et al. Spinal cord injury causes rapid osteoclastic resorption and growth plate abnormalities in growing rats (SCI-induced bone loss in growing rats). *Osteoporos Int*. 2008;19(5):645–52.
30. Wolfe MS, Klein L. Sex differences in absolute rates of bone resorption in young rats: appendicular versus axial bones. *Calcif Tissue Int*. 1996;59(1):51–7.
31. Turiel M, Sitia S, Cicala S, et al. Robotic treadmill training improves cardiovascular function in spinal cord injury patients. *Int J Cardiol*. 2011;149(3):323–9.
32. Ditor DS, Macdonald MJ, Kamath MV, et al. The effects of body-weight supported treadmill training on cardiovascular regulation in individuals with motor-complete SCI. *Spinal Cord*. 2005;43(11):664–73.
33. Behnke BJ, Ramsey MW, Stabley JN, et al. Effects of aging and exercise training on skeletal muscle blood flow and resistance artery morphology. *J Appl Physiol (1985)*. 2012;113(11):1699–708.
34. Stabley JN, Moningka NC, Behnke BJ, Delp MD. Exercise training augments regional bone and marrow blood flow during exercise. *Med Sci Sports Exerc*. 2014;46(11):2107–12.
35. Panisset MG, Galea MP, El-Ansary D. Does early exercise attenuate muscle atrophy or bone loss after spinal cord injury? *Spinal Cord*. 2016;54(2):84–92.
36. Soleyman-Jahi S, Yousefian A, Maheronnaghsh R, et al. Evidence-based prevention and treatment of osteoporosis after spinal cord injury: a systematic review. *Eur Spine J*. 2018;27(8):1798–814.
37. Burr DB, Robling AG, Turner CH. Effects of biomechanical stress on bones in animals. *Bone*. 2002;30(5):781–6.
38. Lichy AM, Groah S. Asymmetric lower-limb bone loss after spinal cord injury: case report. *J Rehabil Res Dev*. 2012;49(2):221–6.
39. Ogilvie C, Bowker P, Rowley DI. The physiological benefits of paraplegic orthotically aided walking. *Paraplegia*. 1993;31(2):111–5.
40. Mobarake BG, Banitalebi E, Ebrahimi A, Ghafari M. Effects of progressive locomotor treadmill compared to conventional training on bone mineral density and bone remodeling in paraplegia. *Middle East J Rehabil Health Stud*. 2017;4(1):e37732.
41. Giangregorio LM, Hicks AL, Webber CE, et al. Body weight supported treadmill training in acute spinal cord injury: impact on muscle and bone. *Spinal Cord*. 2005;43(11):649–57.
42. Giangregorio LM, Webber CE, Phillips SM, et al. Can body weight supported treadmill training increase bone mass and reverse muscle atrophy in individuals with chronic incomplete spinal cord injury? *Appl Physiol Nutr Metab*. 2006;31(3):283–91.
43. Ko FC, Mortreux M, Riveros D, Nagy JA, Rutkove SB, Bouxsein ML. Dose-dependent skeletal deficits due to varied reductions in mechanical loading in rats. *NPJ Microgravity*. 2020;6:15.
44. Stabley JN, Prisby RD, Behnke BJ, Delp MD. Chronic skeletal unloading of the rat femur: mechanisms and functional consequences of vascular remodeling. *Bone*. 2013;57(2):355–60.
45. Prisby RD, Behnke BJ, Allen MR, Delp MD. Effects of skeletal unloading on the vasomotor properties of the rat femur principal nutrient artery. *J Appl Physiol (1985)*. 2015;118(8):980–8.
46. Colleran PN, Wilkerson MK, Bloomfield SA, Suva LJ, Turner RT, Delp MD. Alterations in skeletal perfusion with simulated microgravity: a possible mechanism for bone remodeling. *J Appl Physiol (1985)*. 2000;89(3):1046–54.
47. Marenzana M, Arnett TR. The key role of the blood supply to bone. *Bone Res*. 2013;1(3):203–15.
48. Ding WG, Yan WH, Wei ZX, Liu JB. Difference in intraosseous blood vessel volume and number in osteoporotic model mice induced by spinal cord injury and sciatic nerve resection. *J Bone Miner Metab*. 2012;30(4):400–7.
49. Barou O, Mekraldi S, Vico L, Boivin G, Alexandre C, Lafage-Proust MH. Relationships between trabecular bone remodeling and bone vascularization: a quantitative study. *Bone*. 2002;30(4):604–12.